

Analytical Solution and Frequency Extraction of Iris Problems in Waveguide by Separation of Variables

Tullio Rozzi, *Fellow, IEEE*, Antonio Morini, *Member, IEEE*, Federica Ragusini, and Mauro Mongiardo, *Member, IEEE*

Abstract—The field nearby a thin iris discontinuity can be found in an exact manner by solving the wave equation in an appropriate coordinate system. To this end, it is necessary to select a coordinate system that fits the iris boundary. As an example, capacitive and inductive irises in rectangular waveguides have been solved by considering the Helmholtz equation in the elliptic-cylinder coordinate system. The presence of the waveguide environment is then enforced either by using the aperture field solution in a variational expression of the equivalent shunt susceptance or by taking images.

The advantage of the new solution is that a single term solution, apart from being very accurate and numerically efficient, also contains the correct frequency dependence; thus providing results over the entire band. Moreover, wide-band equivalent circuits with frequency independent elements of the Foster's canonical form descend directly from the field analysis.

I. INTRODUCTION

EQUIVALENT circuits of irises' discontinuities have received considerable attention in the past in view of their usefulness for the design of several waveguide components such as filters, multiplexers, etc. In order to characterize waveguide discontinuities it is advantageous to use variational formulae [1], which provide the sought susceptance in terms of the field on the transverse section containing the iris discontinuity. A better field representation leads to a more efficient evaluation of the susceptance. The crucial point is therefore the choice of the unknown tangential electric field on the aperture, or conversely, of the unknown current on the metallization. Consider for instance, a capacitive window in a rectangular waveguide and its solution in terms of the tangential electric field on the aperture (Fig. 1). Typically, the unknown field is expanded into a set of functions belonging to one of the following classes:

- 1) functions satisfying the wave equation, but not having the correct behavior at the edges, such as $\cos(2n\pi/w)x$;
- 2) functions having the correct behavior at the edges, but not satisfying the wave equation, such as Chebyshev polynomials weighted by an appropriate singular function $T_n(2x/w)(1 - (2x/w)^2)^{-1/2}$ [2];

Manuscript received February 6, 1996; revised October 18, 1996. This work was supported in part by Ministero Università e della Ricerca Scientifica e Tecnologica (MURST).

T. Rozzi and A. Morini are with the Dipartimento di Elettronica ed Automatica, Università di Ancona, I-60131 Ancona, Italy.

M. Mongiardo is with the Istituto di Elettronica, Università di Perugia, I-06100, Perugia, Italy.

F. Ragusini was with the Dipartimento di Elettronica ed Automatica, Università di Ancona, I-60131 Ancona, Italy. She is now with Ente Nazionale Energie Alternative (ENEA), Rome, Italy.

Publisher Item Identifier S 0018-9480(97)00830-2.

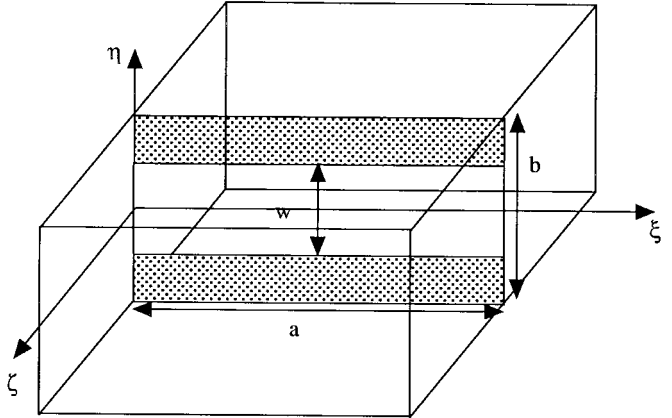


Fig. 1. Capacitive septum in rectangular waveguide.

- 3) very simple functions having neither the correct behavior at the edges nor satisfying the wave equation, such as, pulses, triangular functions, etc.

Although good results can be obtained from all three choices, there are drawbacks. In particular, the first choice requires a large number of expanding functions involving consequently large matrices. Those dimensions are considerably reduced with the second choice, but large apertures still require employing a few functions and the error increases with frequency. The third choice is appreciated for its flexibility, but it also requires still more expanding functions than the former choices. The first and the third sets, moreover, do not produce an accurate description of the field near the edges. Furthermore, since the functions belonging to the above sets do not depend on frequency, that dependence enters the expanding coefficients, which, consequently, have to be calculated at each spot frequency.

A conceptually different approach is proposed in this paper. Instead of expanding the field in terms of one of the above sets, we look for a solution of the wave equation nearby the discontinuity. Such a solution has to *locally* satisfy all the boundary and edge conditions and can be obtained analytically by first neglecting the presence of the waveguide walls. In fact in that case, it is possible to find a coordinate system which fits the boundary conditions of our discontinuity. Such a coordinate system can be found in several cases; for example, those shown in Fig. 2, thus enabling an elegant and effective solution of the iris in an infinite ground plane. As an example, when considering a thin capacitive iris in a rectangular waveguide, we note that the field in the proximity of the iris must satisfy the same boundary conditions as the one present in a

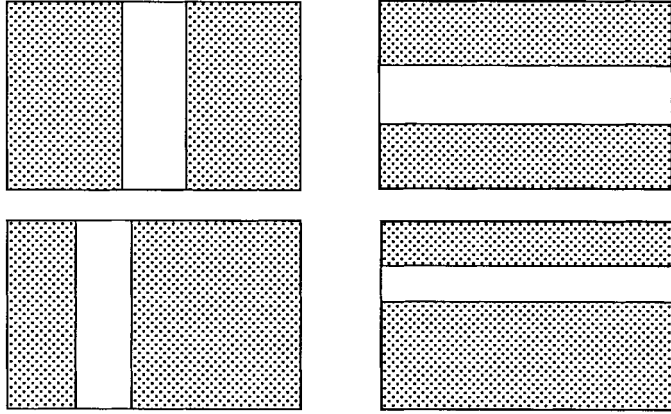


Fig. 2. Some irises which can be analyzed by the proposed method.

slotted metallic plane. The latter structure, however, allows an analytical solution of the Helmholtz equation in the elliptic-cylinder coordinate system. The presence of the waveguide walls is then enforced by employing the above field solution in the appropriate variational formula for the sought susceptance.

The advantages of the proposed approach are that the one term solution not only satisfies the edge conditions, but also has the correct frequency dependence, thus making it particularly easy to extract single and multimode frequency-independent equivalent circuits.

II. APPLICATION OF THE METHOD TO A CAPACITIVE WINDOW

In the capacitive case of Fig. 1, we have a three-components field, namely E_η , E_ζ , H_ξ ; the variational formula for the iris susceptance in this case is given by

$$B(\omega) = 4k_t \frac{\sum_{n=2}^{\infty} \frac{1}{\gamma_n} \left[\int_{-w/2}^{w/2} \cos\left(\frac{n\pi\eta}{b}\right) E_\eta(\eta, \omega) d\eta \right]^2}{\left[\int_{-w/2}^{w/2} E_\eta(\eta, \omega) d\eta \right]^2} \quad (1)$$

with

$$k_t = \sqrt{k_0^2 - \left(\frac{\pi}{a}\right)^2}$$

$$\gamma_n = \sqrt{\left(\frac{n\pi}{b}\right)^2 - k_t^2}.$$

In order to solve this problem we consider an appropriate elliptical coordinate system, centered on the slot, as shown in Fig. 3:

$$x = \frac{w}{2} \cosh \mu \cos \phi \quad (2)$$

$$y = \frac{w}{2} \sinh \mu \sin \phi. \quad (3)$$

The above coordinate system is related to that inside the guide as $E_\eta = E_x$, $E_\zeta = E_y$, and $H_\xi = H_z$.

It is convenient to derive the unknown electric field from the potential $\psi(x, y) = H_z(x, y)$ which, with reference to Fig. 3, yields the TE to z electric field in the slot as

$$E_\eta = E_\phi(\mu = 0) = \frac{j\omega\mu_0}{w/2 \sin \phi} \partial_\mu H_z. \quad (4)$$

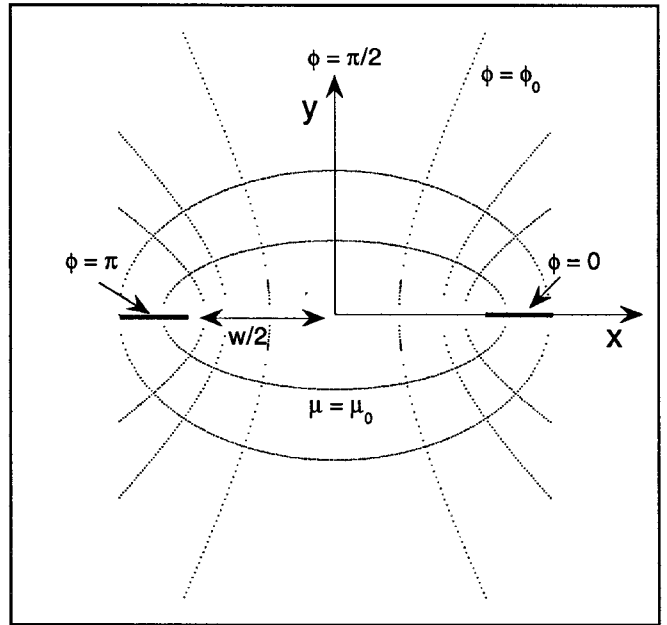


Fig. 3. Elliptical coordinates.

The wave equation for the potential $\psi(x, y)$ becomes the Mathieu equation:

$$[\partial_\mu^2 + \partial_\phi^2 + h^2(\cosh^2 \mu - \cos^2 \phi)]\psi = 0 \quad (5)$$

with

$$h = \frac{k_0 w}{2} \quad (6)$$

under boundary conditions, corresponding to even excitation:

$$\psi(\phi, 0) = 0 \text{ on the iris aperture} \quad \mu = 0 \quad (7)$$

$$\partial_\phi \psi(\pi, \mu) = \partial_\phi \psi(0, \mu) = 0 \text{ on the iris metallization.} \quad (8)$$

In a neighborhood of the aperture, the solutions of (5) with boundary conditions (7) and (8) are of the type:

$$\psi(\mu, \phi) = S_{en}(h, \phi) P_{en}(h, \mu), \quad n = 0, 2, 4, \dots \quad (9)$$

$S_{en}(h, \phi)$ are called periodic Mathieu functions of the first kind, whereas $P_{en}(h, \mu)$ are combinations of Mathieu functions of the second kind [3] and [4]. Their expressions are, respectively,

$$S_{en}(q, \phi) = \frac{1}{\sqrt{\pi}} \sum_{r=0}^{\infty} A_{2r}^n(q) \cos(2r\phi) \quad (10)$$

where $q = h^2/4$ and the coefficients A_{2r}^n can be found in [5]

$$P_{en}(h, \mu) = J_{en}(h, \mu) N_{en}(h, 0) - J_{en}(h, 0) N_{en}(h, \mu) \quad (11)$$

with

$$P_{en}(h, 0) = 0 \quad P'_{en}(h, 0) = 1.$$

The functions just introduced exactly satisfy the wave equation and boundary conditions near the window forming a set of slot eigenmodes, whereas the influence of the waveguide side walls

still has to be accounted for. This is done by using the above functions as trial fields in the variational expression of the equivalent shunt susceptance B of the capacitive window.

Therefore, when considering just the first slot eigenmode, we obtain

$$E_\eta(\eta, \omega) = \frac{E_0}{\sin \phi} \sum_{r=0}^{\infty} A_{2r}^0(q\omega) \cos(2r\phi) \quad (12)$$

where E_0 is the field amplitude. It is worth noting that (12), while yielding the correct singularity of the field at the edges of the type $r^{-1/2}$, is also a solution of the wave equation.

By noting that [5, p. 402]

$$\begin{aligned} & \int_{-w/2}^{w/2} \cos\left(\frac{n\pi\eta}{b}\right) E_\eta(\eta, \omega) d\eta \\ &= \frac{E_0 w \pi}{2} \sum_{r=0}^{\infty} A_{2r}^0(q) (-1)^r J_{2r}\left(\frac{n\pi w}{2b}\right) \end{aligned} \quad (13)$$

the final expression of the susceptance is obtained:

$$B(\omega) = \frac{4k_t}{(A_0^0)^2} \sum_{n=2}^{\infty} \frac{1}{\gamma_n} \left[\sum_{r=0}^{\infty} A_{2r}^0(q) (-1)^r J_{2r}\left(\frac{n\pi w}{2b}\right) \right]^2. \quad (14)$$

Expression (14) can be computed very quickly, since the inner series takes just two to three terms to converge. It is also noted that just one Mathieu function is sufficient for obtaining accurate results even for quite large apertures. In this case, however, it is convenient to deal with currents on the iris, still obtained from the solution of the Helmholtz equation in elliptic-cylinder coordinates. For asymmetrical irises the first series in (14) is modified retaining even terms and using two Mathieu functions at most. Multiple slots can be dealt with in an analogous manner

III. THE INDUCTIVE WINDOW

The geometry of the inductive window and its coordinate system are shown in Fig. 4. For TE_{n0} polarization the iris can be seen as a slot on a ground plane excited in the TM^z -polarization (Fig. 3). The appropriate elliptical coordinate system centered on the slot is also shown in Fig. 3:

$$x = \frac{w}{2} \cosh \mu \cos \phi \quad (15)$$

$$y = \frac{w}{2} \sinh \mu \sin \phi. \quad (16)$$

The wave equation for the potential $\psi(x, y) = E_z(x, y)$ is the same as (5) under boundary conditions corresponding to even excitation

$$\partial_\mu \psi(\phi, 0) = 0 \text{ on the iris aperture } \mu = 0 \quad (17)$$

$$\psi(\pi, \mu) = \psi(0, \mu) = 0 \text{ on the iris metallization.} \quad (18)$$

In the neighborhood of the aperture the solutions of (5) with boundary conditions as in (17)–(18) are of the type

$$\psi(\mu, \phi) = S_{on}(h, \phi) P_{on}(h, \mu), \quad n = 1, 3, 5, \dots \quad (19)$$

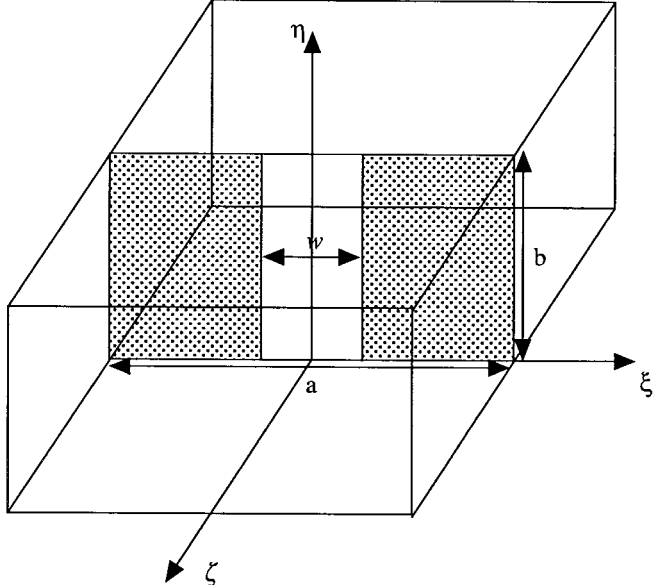


Fig. 4. Inductive window in rectangular waveguide.

where

$$P_{on}(h, \mu) = J_{on}(h, \mu) N'_{on}(h, 0) - J'_{on}(h, 0) N_{on}(h, \mu) \quad (20)$$

with

$$P_{on}(h, 0) = 1 \quad P'_{on}(h, 0) = 0.$$

The functions just introduced exactly satisfy the boundary conditions near the window, forming the set of the slot eigenmodes, whereas the influence of the side walls has still to be accounted for. This is done by using the above functions as trial fields in the variational expression of the equivalent shunt susceptance B of the inductive window, this is,

$$B(\omega) = \frac{2 \sum_{n=3,5}^{\infty} b_{on} \left[\int_{-w/2}^{w/2} \phi_n(\xi) E_\eta(\xi, \omega) d\xi \right]^2}{\left[\int_{-w/2}^{w/2} \phi_1(\xi) E_\eta(\xi, \omega) d\xi \right]^2} \quad (21)$$

where $-jb_{0n}$ is the modal admittance, ϕ_n the n th modal distribution, E_η the trial field. In particular, using just one function, the first odd TM slot eigenmode, we obtain

$$E_\eta(\xi, \omega) = E_0 \sum_{r=0}^{\infty} B_{2r+1}^1(q) \sin[(2r+1)\phi] \quad (22)$$

where E_0 is the field amplitude, $q = h^2/4$, and the coefficients B_{2r+1}^1 can be found in [5]. Observing that [5, p. 402]

$$\int_{-w/2}^{w/2} \phi_n(\xi) E_\eta(\xi, \omega) d\xi = \frac{E_0}{\sqrt{\pi}} \frac{a}{n} \sum_{r=0}^{\infty} \mathcal{B}_r(q) J_{2r+1}\left(\frac{n\pi w}{2a}\right) \quad (23)$$

where $\mathcal{B}_r(q) = B_{2r+1}^1(q)(2r+1)(-1)^r$.

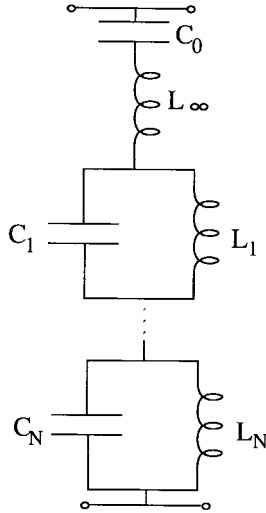


Fig. 5. Foster's equivalent circuit of a realizable reactance.

The final expression of the susceptance becomes

$$B(\omega) = \frac{2 \sum_{n=3,5}^{\infty} b_{on} \left[\frac{1}{n} \sum_{r=0}^{\infty} \mathcal{B}_r(q) J_{2r+1} \left(\frac{n\pi w}{2a} \right) \right]^2}{\left[\sum_{r=0}^{\infty} \mathcal{B}_r(q) J_{2r+1} \left(\frac{\pi w}{2a} \right) \right]^2}. \quad (24)$$

As for the capacitive case, the above expression is computed very quickly since the inner series takes just two to three terms to converge. Therefore, the numerical effort of the above choice is comparable with that required by using just one basic function which satisfies the edge conditions, (i.e., belonging to the second group mentioned in Section I). Moreover, as will be shown in the next section, just one Mathieu function is sufficient for obtaining accurate results even for quite large apertures, noticeably extending the flexibility of the solution.

IV. FREQUENCY EXTRACTION

It is well known that a lossless reciprocal two-port admits the equivalent circuit representation shown in Fig. 5, also known as Foster's form. The correspondent reactance holds:

$$X(\omega) = \omega L_0 - \frac{1}{\omega C_0} + \omega \sum_{j=1}^{\infty} \left[\frac{L_j}{1 - \left[\frac{\omega}{\omega_j} \right]^2} - L_j \right] \quad (25)$$

where

$$\begin{aligned} \bar{\omega} &= \frac{\beta a}{\pi} \\ L_0 &= L_{\infty} + \sum_{j=1}^{\infty} L_j. \end{aligned} \quad (26)$$

For a thin inductive window, we also set $1/C_0 = 0$. The expression of the equivalent inductance is, therefore, obtained

$$L(\omega) = L_0 + \sum_{j=1}^{\infty} \frac{\omega L_j}{1 - \left[\frac{\omega}{\omega_j} \right]^2} - L_j. \quad (27)$$

Starting now from the analytical expression (24), it is immediate to recover the expression of the equivalent inductance associated to the reactance (26):

$$L(\bar{\omega}) = \frac{\left[\sum_{r=0}^{\infty} \mathcal{B}_r(q) J_{2r+1} \left(\frac{\pi w}{2a} \right) \right]^2}{\sum_{n=3,5}^{\infty} \frac{2\sqrt{n^2 - 1 - \bar{\omega}^2}}{n^2} \left[\sum_{r=0}^{\infty} \mathcal{B}_r(q) J_{2r+1} \left(\frac{n\pi w}{2a} \right) \right]^2} \quad (28)$$

where, we have made explicit the form of the normalized modal susceptance $b_{0n}(\bar{\omega}) = \sqrt{n^2 - 1 - \bar{\omega}^2}/\bar{\omega}$. The quasi-static contribution is then obtained by setting $\bar{\omega} = 0$:

$$L_0 = \frac{\left[\sum_{r=0}^{\infty} \mathcal{B}_r(\bar{\omega} = 0) J_{2r+1} \left(\frac{\pi w}{2a} \right) \right]^2}{\sum_{n=3,5}^{\infty} \frac{2\sqrt{n^2 - 1}}{n^2} \left[\sum_{r=0}^{\infty} \mathcal{B}_r(\bar{\omega} = 0) J_{2r+1} \left(\frac{n\pi w}{2a} \right) \right]^2}. \quad (29)$$

Since the poles $\bar{\omega}_j$ of the equivalent inductance (29) coincide with the zeros of the denominator of expression (25), they can be obtained in a straightforward manner and with great accuracy by solving the equation:

$$\begin{aligned} \sum_{n=3,5}^{\infty} \frac{2\sqrt{n^2 - 1 - \bar{\omega}^2}}{n^2} \left[\sum_{r=0}^{\infty} \mathcal{B}_r(\bar{\omega}) J_{2r+1} \left(\frac{n\pi w}{2a} \right) \right]^2 \\ = K(\bar{\omega}^2 - \bar{\omega}_1^2)(\bar{\omega}^2 - \bar{\omega}_2^2) \cdots (\bar{\omega}^2 - \bar{\omega}_N^2). \end{aligned} \quad (30)$$

Finally the residues L_j are extracted by comparing (25) and (30), thus obtaining

$$L_j = -\frac{\left[\sum_{r=0}^{\infty} \mathcal{B}_r(\bar{\omega}) J_{2r+1} \left(\frac{\pi w}{2a} \right) \right]^2}{2K\bar{\omega}_j^2(\bar{\omega}_j^2 - \bar{\omega}_1^2) \cdots (\bar{\omega}_j^2 - \bar{\omega}_{j-1}^2) \cdots (\bar{\omega}_j^2 - \bar{\omega}_N^2)}. \quad (31)$$

A further simplification is achieved by truncating the frequency dependence in such a way as to consider the terms up to $\bar{\omega}^2$. Under this approximation we obtain

$$B_1^1(\bar{\omega}) \approx 1 \quad (32)$$

$$B_3^1(\bar{\omega}) \approx -\frac{1}{32} \left(\frac{\pi w}{2a} \right)^2 (\bar{\omega}^2 + 1). \quad (33)$$

Therefore, it is immediate to recover

$$L_0 = \frac{\left[J_1 \left(\frac{\pi w}{2a} \right) + \frac{3}{32} \left(\frac{\pi w}{2a} \right)^2 J_3 \left(\frac{\pi w}{2a} \right) \right]^2}{\sum_{n=3,5}^{\infty} \frac{2\sqrt{n^2 - 1}}{n^2} \left[J_1 \left(\frac{n\pi w}{2a} \right) + \frac{3}{32} \left(\frac{\pi w}{2a} \right)^2 J_3 \left(\frac{n\pi w}{2a} \right) \right]^2} \quad (34)$$

$$L_1 = -\frac{\left[J_1 \left(\frac{\pi w}{2a} \right) + \frac{3}{32} \left(\frac{\pi w}{2a} \right)^2 J_3 \left(\frac{\pi w}{2a} (\bar{\omega}_1^2 + 1) \right) \right]^2}{2K\bar{\omega}_1^2(\bar{\omega}_1^2 - \bar{\omega}_2^2)(\bar{\omega}_1^2 - \bar{\omega}_3^2) \cdots (\bar{\omega}_1^2 - \bar{\omega}_N^2)}. \quad (35)$$

The resulting equivalent circuit is finally shown in Fig. 6.

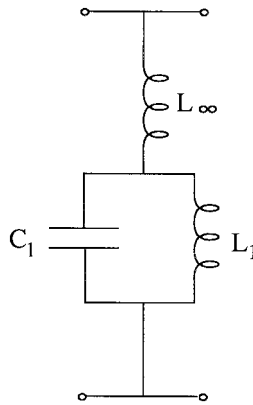


Fig. 6. Final equivalent circuit of the inductive window.

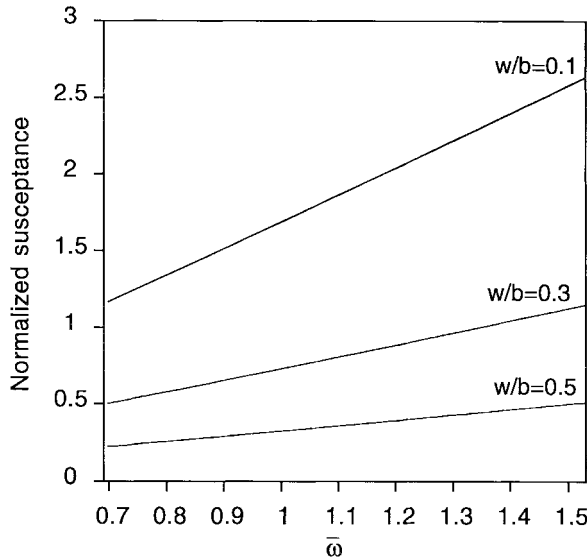


Fig. 7. E-window comparison between the susceptances deriving from one Mathieu function and those calculated with three Chebyshev polynomials. The curves are indistinguishable.

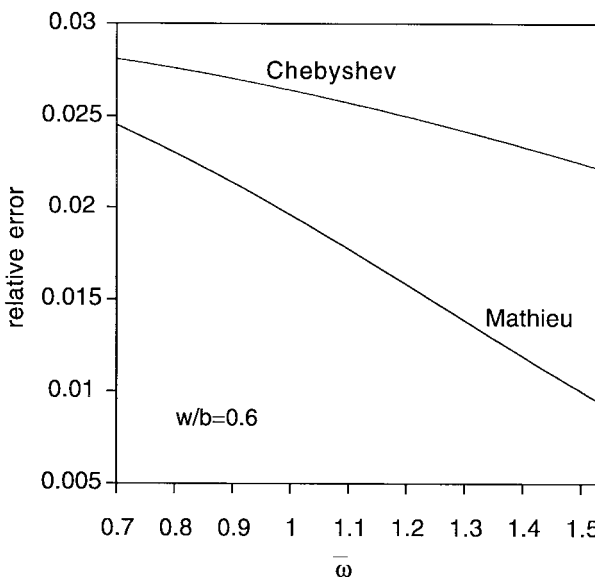


Fig. 8. E-window comparison between the error using just one Mathieu function and the error calculated with one Chebyshev polynomial.

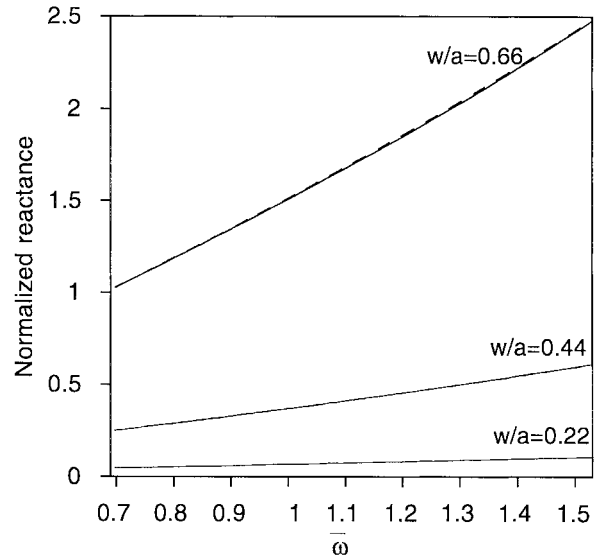


Fig. 9. H-window comparison between the reactances deriving from one Mathieu function with those calculated with three Chebyshev polynomials. The curves are indistinguishable.

V. RESULTS

The accuracy of the present approach, using just a single slot eigenmode, was checked by comparing our results with those obtained employing a set of Chebyshev polynomials weighted by the correct edge condition [2]. Under TE_{10} excitation, for the latter to achieve adequate accuracy it is necessary to consider three basis functions, resulting in a Green's matrix of dimensions 3×3 . The computation time for that solution is about four times greater than that required by the proposed one. For instance, the computation of the susceptance for the inductive case employing three Chebyshev polynomials computed at 40 frequency spots takes 47 s to run on a DIGITAL α 3000/300X versus 11 s required by the present solution. The latter is drastically reduced when the derivation of the equivalent circuit is performed. In that case less than 1 s is required to analyze the window at 100 frequency spots. It is also noted that the process of equivalent circuit extraction is greatly simplified with respect to [6].

A. Capacitive Window

Fig. 7 shows a comparison between the susceptances obtained when using three Chebyshev polynomials and just one Mathieu function, considering three different windows, and up to 50% of the waveguide height versus frequency. The results are indistinguishable.

Results deteriorate somewhat for wider aperture. In that case it is convenient to reformulate the problem in terms of currents on the flanges, employing of course, the same expanding functions. In order to appreciate the accuracy of the approximation with respect to frequency, Fig. 8 compares the errors involved when considering the first Mathieu function and the first Chebyshev polynomial for a 60% height window. It is apparent that for the former the error is considerably smaller and decreasing with frequency, as the field is better confined to the slot.

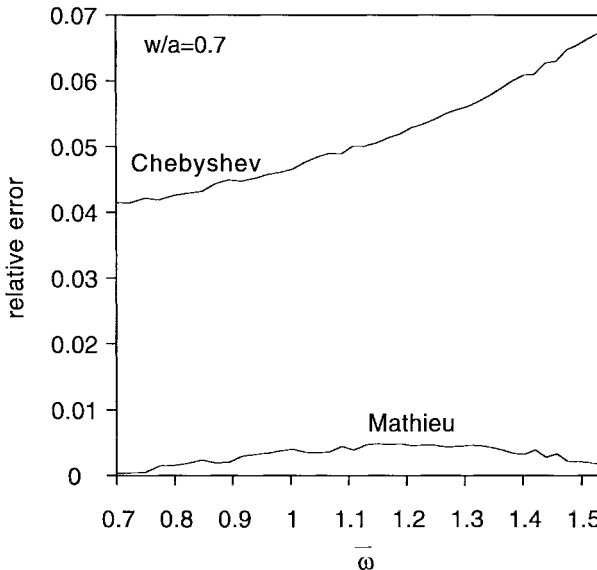


Fig. 10. H-window comparison between the error using just one Mathieu function and the error calculated with one Chebyshev polynomial. The curves are indistinguishable.

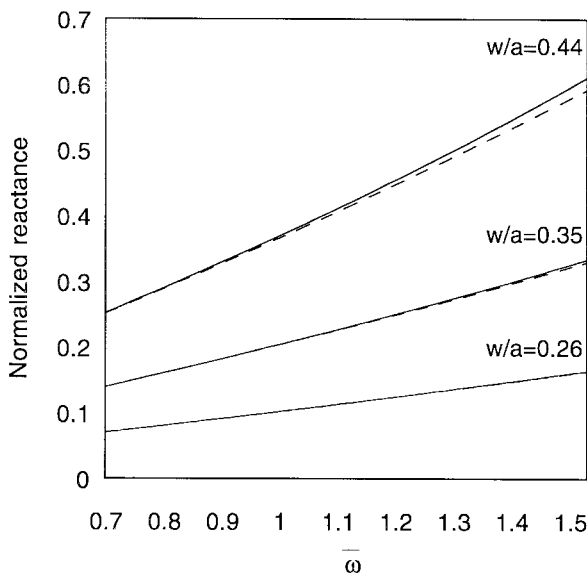


Fig. 11. Comparison between the reactances deriving from the equivalent circuit (continuous line) and the reactances calculated with three Chebyshev polynomials (dashed line).

B. Inductive Window

Fig. 9 shows a comparison between the reactances obtained by considering three different windows of aperture up to 66% of the waveguide width versus frequency. In this case too, for still wider windows it is more expedient to reformulate the problem in terms of currents on the flanges. In order to appreciate the accuracy of the approximation with respect to frequency, Fig. 10 compares the errors involved when considering the first Mathieu function and the first Chebyshev polynomial for a 70% wide window. It is apparent that for the former the error is considerably smaller and quite constant over the whole band, whilst for the latter the error increases with frequency.

Finally, Fig. 11 shows a comparison between true reactance values and those obtained from the equivalent circuit of Fig. 6.

VI. CONCLUSION

We introduce the use of appropriate combinations of the Mathieu functions as a new expanding set for the electric field across a thin iris or for the current on a thin septum. This set, satisfying edge conditions as well as the wave equation, provides the most effective trial field so far in the variational solution of this class of problems.

REFERENCES

- [1] J. Schwinger and D. Saxon, *Discontinuities in Waveguides*. New York: Gordon and Breach, 1968.
- [2] T. Rozzi, "A new approach to the network modeling of capacitive irises and steps in waveguide," *Circuit Theory Appl.*, vol. 3, pp. 339-354, 1975.
- [3] A. El-Sherbiny, "Cutoff wavelengths of ridged, circular, and elliptic guides," *IEEE Trans. Microwave Theory Tech.*, vol. MTT-21, pp. 7-12, Jan. 1973.
- [4] P. Morse and H. Feshback, *Methods of Theoretical Physics*. New York: McGraw-Hill, 1953.
- [5] S. Gradshteyn and I. M. Rhyzik, *Table of Integrals Series, and Products*. New York: Academic Press, 1965.
- [6] T. Rozzi and W. G. Mecklenbrauker, "Wide-band network modeling of interacting inductive irises and steps," *IEEE Trans. Microwave Theory Tech.*, vol. MTT-23, pp. 235-245, Feb. 1975.

Tullio Rozzi (M'66-SM'74-F'90) received the Dottore degree in physics from the University of Pisa, Tuscany, Italy, in 1965, the Ph. D. degree in electronic engineering from Leeds University, Leeds, U.K., in 1968, and the D. Sc. degree from the University of Bath, Bath, U.K., in 1987.

From 1968 to 1978 he was a Research Scientist at the Philips Research Laboratories, Eindhoven, the Netherlands. In 1975, he spent one year at the Antenna Laboratory, University of Illinois, Urbana. In 1978 he was appointed the Chair of Electrical Engineering at the University of Liverpool, Liverpool, U.K. and was subsequently appointed, in 1981, to the Chair of Electronics and Head of the Electronics Group at the University of Bath where he also held the responsibility of Head of the School of Electrical Engineering on an alternate three-year basis. Since 1988 he has been Professor of Antennas in the Department of Electronics and Control, University of Ancona, Ancona, Italy, while remaining a Visiting Professor at Bath University. Since 1995 he holds the responsibility of Head of the Department of Electronics and Control, University of Ancona.

Dr. Rozzi is a Fellow of the Institution of Electrical Engineers (IEE), U.K., and IEE Council Representative for Italy. In 1975 he was awarded the Microwave Prize by the IEEE Microwave Theory and Technique Society.

Antonio Morini (M'94) was born in Italy in 1962. He received the Laurea degree in electrical engineering (summa cum laude) and the Ph.D. degree in electromagnetism from the University of Ancona, Ancona, Italy, in 1987 and 1992, respectively.

Since 1992 he has been an Assistant Professor with the Department of Electronics and Automatics at the University of Ancona, Ancona, Italy. His research is mainly devoted to the modeling and synthesis of passive millimetric components such as filters, multiplexers, and antennas.



Federica Ragusini was born in Italy in 1970. She received the Laurea degree in electronic engineering from the University of Ancona, Ancona, Italy, in 1995.

She presently works as a Researcher with Ente Nazionale Energie Alternative (ENEA), Rome, Italy. Her research activity concerns the development of an analytical method for the characterization of waveguide components.



Mauro Mongiardo (M'91) received the Laurea degree from the University of Rome (summa cum laude) and the Ph.D. degree from the University of Bath, Bath, U.K., in 1983 and 1991, respectively.

Since 1983 he has worked on microwave radiometry, inverse problems, and in the experimental validation of a four-channel radiometer developed for temperature retrieval of biological bodies. He has been a Visiting Scientist at the University of Victoria, B.C., Canada, working on time-domain analysis of monolithic microwave integrated circuits (MMIC's).

He is presently an Associate Professor at the University of Perugia, Perugia, Italy. He is interested in the modeling and computer-aided design of microwave and millimeter-wave guiding structures and antennas, and in the modeling of discontinuities in MMIC's. In 1988 he was the recipient of a NATO-CNR research scholarship during which he was a Visiting Researcher at the University of Bath, Bath, U.K.